Nanoscale electrochemical imaging

DOI: 10.1002/anie.200((will be filled in by the editorial staff))

Definitive Evidence for Fast Electron Transfer at Basal Plane Graphite from High Resolution Electrochemical Imaging**

*Stanley C.S. Lai[†], Anisha N. Patel[†], Kim McKelvey and Patrick R. Unwin**

There is presently intense activity in electrochemical applications of novel sp^2 carbon materials, such as carbon nanotubes[1] and graphene,[2] which has led to a resurgence of interest in the intrinsic electrochemical properties of highly oriented pyrolytic graphite (HOPG), to which these materials are often compared.[1] The traditional consensus, deduced mostly from macroscopic cyclic voltammetry measurements (typically on areas > 0.1 cm^2) is that the electron transfer (ET) activity of HOPG is dominated by the step edges,[1,2g,3] with the basal plane showing very low[4] to no[5] electroactivity. However, the scale of these measurement necessarily means that HOPG basal planes and step edges are probed simultaneously,[3a,4 6] making it difficult to separate their individual reactivities. Furthermore, there are significant variations in reported HOPG electroactivity,[1c,3a-c,4-7] which has been attributed to each HOPG cleaved surface showing different quality (primarily step edge density). Consequently, various methods have been proposed to determine the step or defect density of cleaved HOPG. [1c,3a-c,4-7] However, the methods used hitherto are either microscopic and can only access a tiny fraction of the surface that is probed by macroscopic electrochemistry,[7c,7d,8] or are indirect measurements of surface quality,[4,6b,6c,7d] making it difficult to correlate HOPG surface structure and ET activity.

In this Communication, we report significant advances in the newly developed scanning electrochemical cell microscopy (SECCM) technique,[9] which allows spatially resolved electrochemical imaging on a scale where the HOPG basal plane can be studied directly in isolation from step edges, and where the response also informs on the location of the measurement (basal surface vs. step edge). By further correlating high-resolution electrochemical measurements with atomic force microscope (AFM) images over the same area, we show unambiguously that the HOPG basal plane supports fast ET activity and conclude that the present (textbook)[10] model for the electroactivity of carbon-based materials requires radical revision.

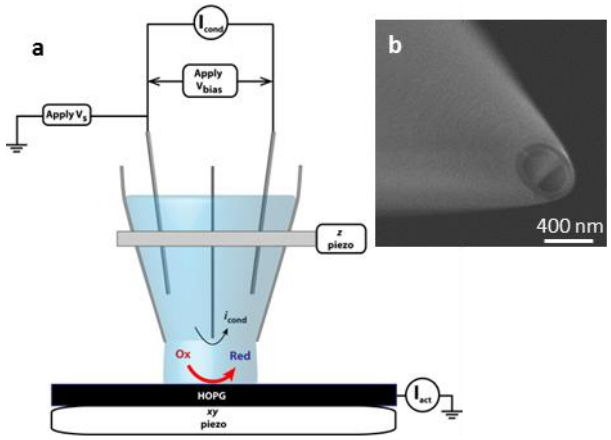

Figure 1 Principles of scanning electrochemical cell microscopy (SECCM). (a) Schematic of the SECCM set-up. (b) SEM image of the end of a pipet.

The SECCM system is shown schematically in Figure 1a and is discussed in detail elsewhere.[9] In brief, a dual-channel glass capillary was pulled to a sharp point (300 - 400 nm; Figure 1b). Each channel was filled with an aqueous electrolyte solution and an Ag/AgCl quasi-reference counter electrode (QRCE). The liquid meniscus at the end of the pipet was brought into gentle contact with the HOPG sample, forming a positionable and moveable nanoelectrochemical cell with the contacted area of the HOPG as the working electrode. The pipet itself never touches the sample. A potential bias (0.5 V) was applied between the two QRCEs and a small oscillation (20 nm peak amplitude, 233.6 Hz herein) was imposed on the *z*-position of the tip, giving rise to a conductance current across the meniscus with an alternating current (AC) component due to periodic changes in the meniscus height. Using the AC as a set-point, the tip was scanned over the surface with a constant tip-to-substrate separation. By recording the currents between the QRCEs and at the substrate, and the positions of the piezoelectric positioners, simultaneous maps of local substrate electroactivity and topography are obtained. In this study, all SECCM maps cover 10 x 10 µm areas of HOPG (31 lines of 10 µm, scan rate 0.3 µm s^{-1}). A data point (an average of 512 measurements) was recorded every 30.1 ms, resulting in *ca.* 1100 points per line and over 30,000 individual current measurements in an image. The contact diameter of the meniscus and the substrate was determined to be 220-320 nm (see SI), indicative of a SECCM spatial resolution an order of magnitude smaller than the typical µm-range step spacing on ZYA grade HOPG[11] (used throughout this study, see SI). This allowed the basal plane to be probed in isolation, without influence of step edges.

SECCM maps obtained for the one-electron reduction of $Ru(NH_3)_6^{3+}$ (0.1 M KCl) on HOPG are shown in Figure 2. The topographical map of the surface (Figure 2a) clearly shows parallel steps (also evident from AFM, Figure 2e) across the surface, highlighting the outstanding ability of the technique to accurately track the surface and resolve nanoscale topographical features, despite a slight tilt (~1.5°) on the sample. The steps are especially pronounced in Figure 2b, which shows the AC component of the conductance current (used as the feedback parameter). The sharp lines on this 'error' map indicate a transient change in the feedback as the liquid meniscus comes into contact with a step, which we

[†] These authors contributed equally.

[*] Dr. S.C.S. Lai, A.N. Patel, K. McKelvey, Prof. Dr. P.R. Unwin
Department of Chemistry
University of Warwick
Coventry CV4 7AL, United Kingdom
E-mail: P.R.Unwin@warwick.ac.uk

K. McKelvey
MOAC doctoral training centre
University of Warwick
Coventry CV4 7AL

[**] We are grateful to the following for support of this work: the European Research Council (ERC-2009-AdG 247143-QUANTIF), and Marie Curie IEF (project 275450 "VISELCAT") under the EU's Seventh Framework Programme (FP7/2007-2013) for funding to SCSL, EPSRC for studentships to KM (MOAC/DTC) and ANP (Analytical Fund EP/F064861/1e). We thank Mr. Petr Dudin for help with artwork preparation. Some equipment used in this research was obtained through Birmingham Science City with support from Advantage West Midlands and the European Regional Development Fund.

Supporting information for this article is available on the WWW under http://www.angewandte.org or from the author.

attribute to different wetting properties of the basal plane and the step edge (*vide infra*).

A simultaneously recorded map of the surface redox activity at the reversible half-wave (formal) potential (-0.25 V *vs* Ag/AgCl/0.1M KCl), as determined by SECCM voltammetry (SI Figure S3a), shows the currents over the entire surface to be essentially constant at 30.9 ± 1.1 pA (1 σ) (Figure 2c). The step sites show slightly higher currents (2-3%), but this is not necessarily an indicator of higher intrinsic activity, i.e. current density (*vide infra*). Most importantly, in the regions between the steps (where the electrolyte solution is only in contact with the basal surface), the current is at a constant (high) value.

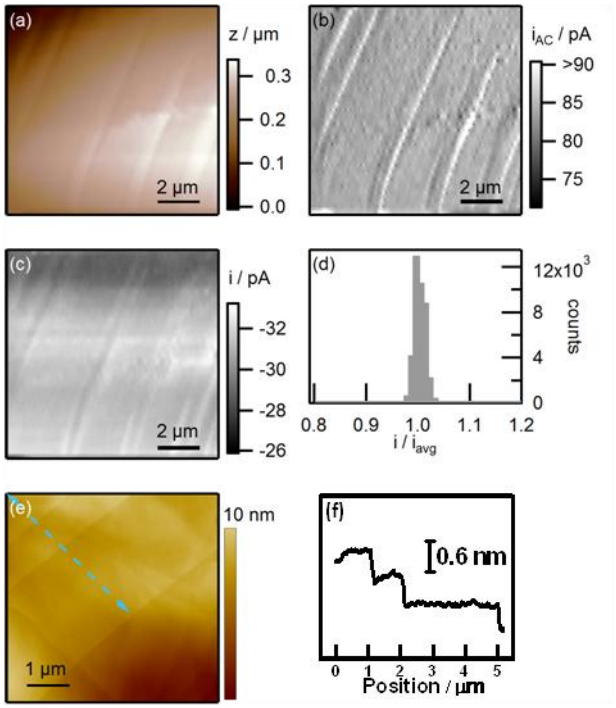

Figure 2 Reduction of 2 mM $Ru(NH_3)_6^{3+}$ at HOPG. SECCM maps of (a) topography (*z*-piezo response), (b) the AC component of the conductance current, (c) surface redox activity recorded at -0.25 V. (d) Normalized activity histogram (see text). (e) AFM image of the area of interest. (f) Line scan along the arrow of the AFM image.

Based on the observed current, an estimate of the standard ET rate constant can be made. The reversible voltammogram for $Ru(NH_3)_6^{3+}$ reduction shows a diffusion limited current of 16 pA (SI Figure S3a) By applying a potential bias of 0.5 V between the two QRCEs the limiting current increased by a factor of 4-5 due to migration. This corresponds to a high mass transport coefficient of ~ 0.5 cm s^{-1}, based on a 300 nm contact diameter. As the currents measured in the SECCM maps at the formal potential are *ca*. 50% of the transport-limited values, it is evident that the surface redox process measured during imaging is fast, and close to reversible, and we can put a conservative lower estimate on the standard ET rate constant of > 0.5 cm s^{-1} for $Ru(NH_3)_6^{3+}$ oxidation on basal plane HOPG. That is to say, the process at HOPG would be entirely reversible to essentially all macroscopic electrochemical techniques, including past CV measurements, purely based on the activity of the basal surface, without needing to consider any activity of the step edges. This is in sharp contrast with the previously reported 'negligible' activity of the basal surface.[1c,5]

These findings are further validated by the other maps obtained simultaneously during imaging, most notably the consistency between all recorded trace and retrace images (SI section S2.b). The spread in redox activity over the image can be evaluated quantitatively (normalized for each line to minimize time effects), as shown by the histogram in Figure 2d. It can clearly be seen that the total spread in surface currents (*ca.* 30,000 data points), is less than 5%, indicating a very homogeneously active surface. After performing SECCM measurements, the imaged area was characterized by AFM (Figure 2e) showing a step spacing ranging between 500 nm to 3 µm (Figure 2f), with mainly monolayer steps present. As the lateral contact of SECCM is an order of magnitude smaller than the (average) step spacing, it is without doubt that during the electrochemical mapping the surface in contact with the electrolyte solution would mostly consist of only the HOPG basal plane. Thus, our data provide unambiguous evidence for the very high ET activity of the basal surface.

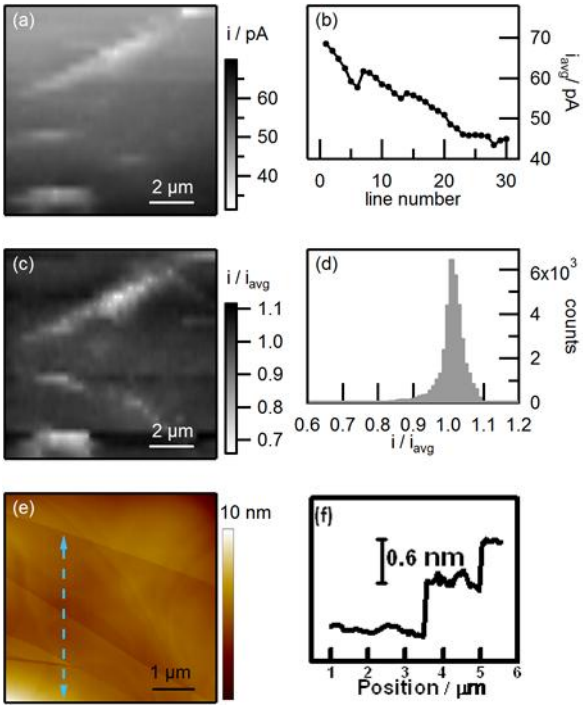

Figure 3 Oxidation of 2 mM $Fe(CN)_6^{4-}$ at HOPG. (a) SECCM surface redox activity map recorded at 0.25 V. (b) Average current of each line scan. (c) Normalized SECCM surface redox activity map (see text). (d) Normalized activity histogram (see text). (e) AFM image of the area of interest. (f) Line scan along the arrow of the AFM image.

We also considered the electrochemical activity of $Fe(CN)_6^{4-/3-}$, a common benchmark redox system often used to study the electrochemical properties of HOPG,[1,3a,3b,4-5,6a,7f] and related sp^2 carbon materials[1c,2h,3b] and originally employed to draw conclusions regarding the relative electroactivity of the basal plane and step sites. SECCM results for the oxidation of 2 mM $Fe(CN)_6^{4-}$ (0.1 M KCl) on HOPG at 0.25 V (*vs* Ag/AgCl/0.1 M KCl) are shown in Figure 3. The potential was chosen based on voltammograms recorded on freshly cleaved HOPG and on HOPG after exposure to air for ~1 hour, being the timescale of a SECCM measurement (SI Figure S3). The limiting current in the absence of migration was 15 pA and 4 – 5 times larger with the applied potential between the QRCEs. The resulting electroactivity map (Figure 3a) shows a clear side-on 'V-shaped' feature consistent with the step sites on the HOPG surfaces (see AFM data, Figure 3e and f). Interestingly, in contrast to the reduction of $Ru(NH_3)_6^{3+}$, these steps display lower currents than the basal plane. Furthermore, a clear deactivation of the overall surface is seen during the timescale of the image (from bottom to top). This decrease is especially clear from the average current of each line (Figure 3b), which dropped by 35% over the course of the image from 69 pA (where the reaction is rapid and close to reversible) to 45 pA. It should again be emphasized that the other simultaneously obtained maps (SI section

S2b) indicate a stable meniscus contact, and that the meniscus is moved during the scan to areas which have not been exposed to the electrolyte solution. This deterioration has been observed in extensive related experiments in our lab and is due a combination of issues which we will expand on in a later paper. For this study, to probe the relative reactivity of basal and step sites in isolation of time effects, a current distribution was obtained by normalizing each line with the average current of that line (Figure 3c and d). Most of the sites display similar activity (within 10%), although a slight tailing towards lower activity can be seen. Looking at the normalized current SECCM map, the regions of below average current are assigned to the step sites. Furthermore, the difference between the step site and basal plane reactivity appears to increase with time, giving rise to the broad distribution of activity in Figure 3d between 0.7 and 1. This increasing difference could be indicative of a preferential deactivation of step sites over basal plane sites with time, similar to metal electrodes.[12] Based on these data, we can only conclude that the HOPG basal plane is highly active for the $Fe(CN)_6^{4-/3-}$ benchmark system, being close to reversible initially, albeit with some complications. This contrasts markedly with previous reports, and it should be noted that previously reported ET standard rate constants (10^{-5} – 10^{-9} cm s^{-1}, averaged for the surface[3a,6b,6c] or 10^{-9} cm s^{-1}, extrapolated for the basal surface[1c,3c]) would have yielded negligible (close to zero) currents at the potential of our high mass transport rate studies. Furthermore, it should be noted that the ET rate constants reported here are consistent with predictions from Marcus theory (> 1 cm s^{-1}).[1b]

Although SECCM clearly illustrates the HOPG basal plane to be highly active, the different currents obtained when imaging directly over step sites is interesting and merits some discussion. We believe this effect is due to the heterogeneous properties of the basal surface versus step edges, resulting in different (nanoscale) wetting and adsorption processes: the excess negative charge on the HOPG step edges[13] could draw in the positively charged $Ru(NH_3)_6^{3+}$ through electrostatic interaction, causing a slight spreading of the meniscus, thereby increasing the contact area. This finding is supported by an increase in conductance current (SI Figure S2.1), which is a good indicator for variances in meniscus size, and the transient surges in the AC (Figure 2b). Due to the increased contact area, the surface current increases, even if the intrinsic activity remains unchanged going over a step edge. In contrast, for the negatively charged $Fe(CN)_6^{4-}$ species, we see the conductance current decrease, suggesting that the meniscus slightly contracts when going over a step site (SI Figure S2.2). These data highlight the high information content of SECCM for structure-function imaging of surfaces and interfaces.

In summary, SECCM has allowed us to study ET at basal plane HOPG under conditions of very high mass transport and high spatial resolution, and where the liquid probe makes a series of fresh measurements across the surface. We have been able to isolate the response of the basal plane, and show unambiguously that ET is fast (close to reversible) for the 2 most studied redox couples. This new view – which overturns more than 2 decades of past research[1,3-8] - not only impacts our understanding of the electroactivity of HOPG, but potentially the properties of related sp^2 materials, such as carbon nanotubes and graphene, illustrating the importance of our findings. Our studies also demonstrate the significant potential of SECCM as a new nanoscale probe of electrochemical and interfacial processes.

Experimental Section

Experimental details are given in the Supporting Information.

Received: ((will be filled in by the editorial staff))
Published online on ((will be filled in by the editorial staff))

Keywords: Electrochemistry, Graphite, Scanning Electrochemical Cell Microscopy (SECCM), Scanning Probe Microscopy, Surface Analysis.

[1] a) I. Dumitrescu, P. R. Unwin, J. V. Macpherson, *Chem. Commun.* **2009**, 6886-6901; b) R. L. McCreery, *Chem. Rev.* **2008**, *108*, 2646-2687; c) C. E. Banks, T. J. Davies, G. G. Wildgoose, R. G. Compton, *Chem. Commun.* **2005**, 829-841; d) M. Pumera, *Chem. Soc. Rev.* **2010**, *39*, 4146-4157.

[2] a) M. Zhou, Y. M. Zhai, S. J. Dong, *Anal. Chem.* **2009**, *81*, 5603-5613; b) Y. Wang, Z. Q. Shi, Y. Huang, Y. F. Ma, C. Y. Wang, M. M. Chen, Y. S. Chen, *J. Phys. Chem. C* **2009**, *113*, 13103-13107; c) L. H. Tang, Y. Wang, Y. M. Li, H. B. Feng, J. Lu, J. H. Li, *Adv. Funct. Mater.* **2009**, *19*, 2782-2789; d) C. S. Shan, H. F. Yang, J. F. Song, D. X. Han, A. Ivaska, L. Niu, *Anal. Chem.* **2009**, *81*, 2378-2382; e) F. Chen, Q. Qing, J. L. Xia, J. H. Li, N. J. Tao, *J. Am. Chem. Soc.* **2009**, *131*, 9908-9909; f) S. Alwarappan, A. Erdem, C. Liu, C. Z. Li, *J. Phys. Chem. C* **2009**, *113*, 8853-8857; g) W. Li, C. Tan, M. A. Lowe, H. D. Abruna, D. C. Ralph, *ACS Nano* **2011**, *5*, 2264-2270; h) A. T. Valota, I. A. Kinloch, K. S. Novoselov, C. Casiraghi, A. Eckmann, E. W. Hill, R. A. W. Dryfe, *ACS Nano* **2011**, *5*, 8809-8815.

[3] a) R. J. Bowling, R. T. Packard, R. L. McCreery, *J. Am. Chem. Soc.* **1989**, *111*, 1217-1223; b) X. B. Ji, C. E. Banks, A. Crossley, R. G. Compton, *ChemPhysChem* **2006**, *7*, 1337-1344; c) T. J. Davies, R. R. Moore, C. E. Banks, R. G. Compton, *J. Electroanal. Chem.* **2004**, *574*, 123-152; d) C. Y. Lee, A. M. Bond, *Anal. Chem.* **2009**, *81*, 584-594.

[4] K. R. Kneten, R. L. McCreery, *Anal. Chem.* **1992**, *64*, 2518-2524.

[5] a) C. E. Banks, R. R. Moore, T. J. Davies, R. G. Compton, *Chem. Commun.* **2004**, 1804-1805; b) T. J. Davies, M. E. Hyde, R. G. Compton, *Angew. Chem.-Int. Edit.* **2005**, *44*, 5121-5126.

[6] a) K. K. Cline, M. T. McDermott, R. L. McCreery, *J. Phys. Chem.* **1994**, *98*, 5314-5319; b) R. J. Rice, R. L. McCreery, *Anal. Chem.* **1989**, *61*, 1637-1641; c) M. T. McDermott, K. Kneten, R. L. McCreery, *J. Phys. Chem.* **1992**, *96*, 3124-3130.

[7] a) R. J. Bowling, R. L. McCreery, C. M. Pharr, R. C. Engstrom, *Anal. Chem.* **1989**, *61*, 2763-2766; b) P. H. Chen, M. A. Fryling, R. L. McCreery, *Anal. Chem.* **1995**, *67*, 3115-3122; c) M. T. McDermott, R. L. McCreery, *Langmuir* **1994**, *10*, 4307-4314; d) R. S. Robinson, K. Sternitzke, M. T. McDermott, R. L. McCreery, *J. Electrochem. Soc.* **1991**, *138*, 2412-2418; e) R. R. Moore, C. E. Banks, R. G. Compton, *Anal. Chem.* **2004**, *76*, 2677-2682; f) C.-Y. Lee, S.-X. Guo, A. M. Bond, K. B. Oldham, *J. Electroanal. Chem.* **2008**, *615*, 1-11; g) J. K. Kariuki, M. T. McDermott, *Langmuir* **1999**, *15*, 6534-6540.

[8] a) K. Ray, R. L. McCreery, *Anal. Chem.* **1997**, *69*, 4680-4687; b) H. Chang, A. J. Bard, *Langmuir* **1991**, *7*, 1143-1153.

[9] a) S. C. S. Lai, P. V. Dudin, J. V. Macpherson, P. R. Unwin, *J. Am. Chem. Soc.* **2011**, *133*, 10744-10747; b) N. Ebejer, M. Schnippering, A. W. Colburn, M. A. Edwards, P. R. Unwin, *Anal. Chem.* **2010**, *82*, 9141-9145.

[10] a) C. G. Zoski, *Handbook of Electrochemistry*, Elsevier B.V., The Netherlands, **2006**; b) R. G. Compton, C. E. Banks, *Understanding Voltammetry*, Imperial College Press Co., United Kingdom, **2011**.

[11] C. G. Williams, M. A. Edwards, A. L. Colley, J. V. Macpherson, P. R. Unwin, *Anal. Chem.* **2009**, *81*, 2486-2495.

[12] a) P. J. Feibelman, S. Esch, T. Michely, *Phys. Rev. Lett.* **1996**, *77*, 2257-2260; b) T. Zambelli, J. Wintterlin, J. Trost, G. Ertl, *Science* **1996**, *273*, 1688-1690.

[13] R. Koestner, Y. Roiter, I. Kozhinova, S. Minko, *J. Phys. Chem. C* **2011**, *115*, 16019-16026.

Entry for the Table of Contents (Please choose one layout)

Nanoscale electrochemical imaging

Stanley C.S. Lai, Anisha N. Patel, Kim McKelvey and Patrick R. Unwin*

_____ **Page – Page**

Definitive Evidence for Fast Electron Transfer at Basal Plane Graphite from High Resolution Electrochemical Imaging

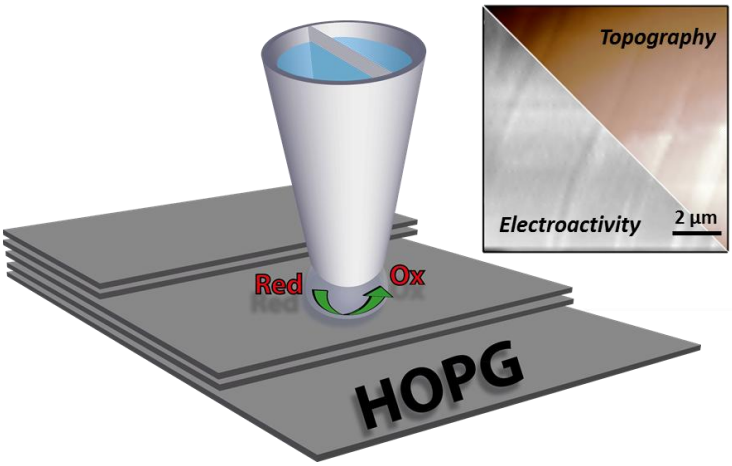

High resolution scanning electrochemical cell microscopy (SECCM) demonstrates that electron transfer at the basal plane of highly oriented pyrolytic graphite (HOPG) is fast and that the current textbook model for HOPG electrochemistry requires radical revision.

Supporting Information for

Definitive Evidence for Fast Electron Transfer at Basal Plane Graphite from High Resolution Electrochemical Imaging

Stanley C.S. Lai‡, Anisha N. Patel‡, Kim McKelvey and Patrick R. Unwin*

Department of Chemistry and MOAC Doctoral Training Centre, University of Warwick, Coventry CV4 7AL, United Kingdom.

‡These authors contributed equally.

* To whom correspondence should be addressed. E-mail: p.r.unwin@warwick.ac.uk.

S.1 ***Basal plane HOPG sample preparation and characterization***

S.1a ***Sample preparation and step edge analysis***.

A fresh surface was revealed by cleaving with scotch tape, as for the majority of studies carried out on HOPG[1] including key studies in which significant conclusions have been drawn relating to the activity of basal plane HOPG.[1b-d,1h,1i,2] From AFM analysis of 20 images taken over areas of 3 – 10 μm on 3 different ZYA grade HOPG samples, the step heights in terms of the number of graphite layers was determined and is shown in Figure S1, which shows that ZYA grade HOPG exhibits predominantly monolayer and bilayer steps, and very low step coverage - among the lowest reported - providing the optimum basal surface on which the density of step edges is minimized. The step density is the length of step per unit area of the surface, while data for step edge coverage takes account of different step heights and represents the total amount of edge plane area within a unit area of the basal surface of HOPG.

Table 1. Characterization of step edges on basal plane HOPG (ZYA)

Step density range ($\mu m\ \mu m^{-2}$) from AFM	0.02 – 0.7
Mean step density ($\mu m\ \mu m^{-2}$) from AFM	0.29 ± 0.2 (*N* = 20)
Step edge coverage on basal plane	Average 0.26% (range 0.03-1%)

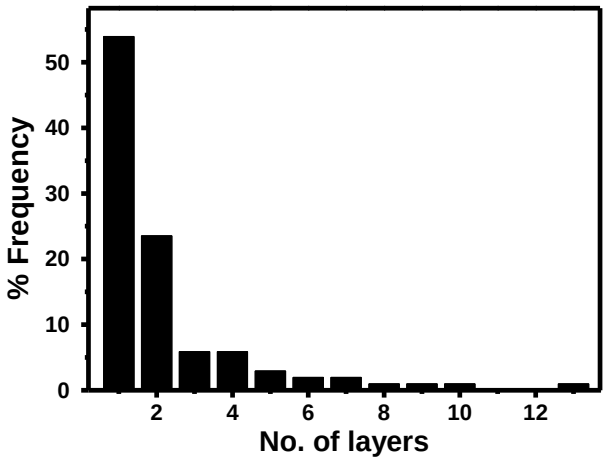

Figure S 1 Histogram of step edge heights on freshly cleaved ZYA grade HOPG

S.1b *Capacitance measurements*

The capacitance of HOPG is often used as a measure for surface quality, although a direct relationship between capacitance and step density remains elusive.[1c-1g,11] For HOPG surfaces prepared by cleaving with adhesive tape, typical values of 2-3 μF cm^{-2} can be found in literature (ref. 1l and references therein). The apparent consensus that the basal plane of HOPG display low (or no) electroactivity was inferred from voltammetric studies of such surfaces.

For our HOPG surfaces, we have found capacitance values ranging from 1.7 to 2.3 μF cm^{-2}, obtained from macroscopic CV measurements in 1 M KCl at 0.1 V s^{-1} on ten freshly cleaved HOPG surfaces. The capacitance values of our surfaces lie well within the accepted range of reported literature values, indicative of a high quality HOPG surface.

S.2 ***Scanning electrochemical cell microscopy (SECCM)***

S.2a ***Setup***

SECCM[3] measurements were performed using a system similar to the one described in ref 4, which allowed independent control of the potential of the substrate and the potential bias between the two quasi-reference counter electrodes (QRCEs) in the tip. The tip was a dual channel probe pulled from borosilicate theta glass capillaries (TGC150-10, Harvard Apparatus) using a CO_2-laser puller (P-2000, Sutter Instruments) to a sharp taper of approximately 400 nm total diameter at the end. The resulting pipet tips were silanized[5] to ensure a hydrophobic outer wall. Each channel was filled with the solution of interest and a chloridized silver wire (99.9%, Mateck). The tip was mounted on a high-dynamic z-piezoelectric positioner (P-753.3CD LISA, Physik Instrumente), while the sample was mounted on a high-precision xy-piezoelectric stage (P-622.2CL PIHera, Physik Instrumente). The entire assembly was installed in a Faraday cage. A sinusoidal oscillation in the z-position of the tip was generated by a lock-in amplifier (SR830, Stanford Research Instruments) and applied to the z-piezoelectric positioner control signal using a home-built signal adder. The lock-in amplifier was also used to identify the AC component of the conductance current when the tip was brought into contact with the surface. Current measurements were performed using high sensitivity home-built current to voltage converters. Tip and sample positioning and data acquisition were performed by using a FPGA card with a LabVIEW 9.0 interface.

S.2b *Contact area determination*

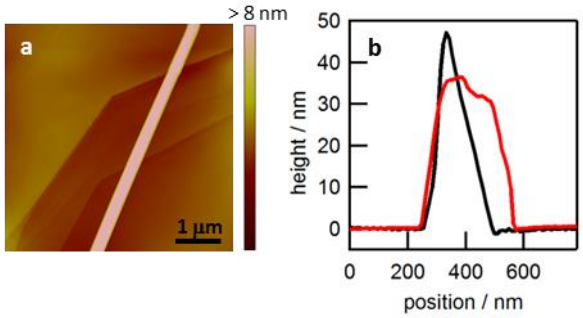

Figure S2.1 Contact area determination of SECCM (a) Tapping mode - atomic force microscope image of polyaniline deposited using SECCM. (d) Cross-sections of deposited polyaniline formed by scanning parallel (red) and perpendicular (black) to the septum in the capillary.

The spatial resolution of SECCM is ultimately determined by the contact area of the meniscus and the substrate, which, in turn, is determined by the tip diameter and local wetting properties. To quantify the contact area, we employed SECCM to electropolymerize aniline in a line-pattern on HOPG, as the width of the line would be a direct measure of the meniscus diameter during the scan. In this case the tip was filled with 1 mM analine in 100 mM KCl and the substrate potential was held at 750 mV relative to the Ag/AgCl QRCE. A tapping mode-atomic force microscope (TM-AFM) image of part of the pattern is shown on a scale comparable to the step spacing on HOPG in Figure S2.1a. The deposited polyaniline is clearly visible and has a uniform width, indicating that the variation in meniscus contact area is minimal as the tip is moved along the surface. From cross-sections of the line (Figure S2.1b), the contact diameter can be determined to be 220 and 320 nm, depending on the relative orientation of the capillary. This is an order of magnitude smaller than the typical step spacing on basal surface HOPG, providing confidence that electrochemical measurements can be made unambiguously on the basal plane, free from the influence of steps.

S.2c *SECCM images*

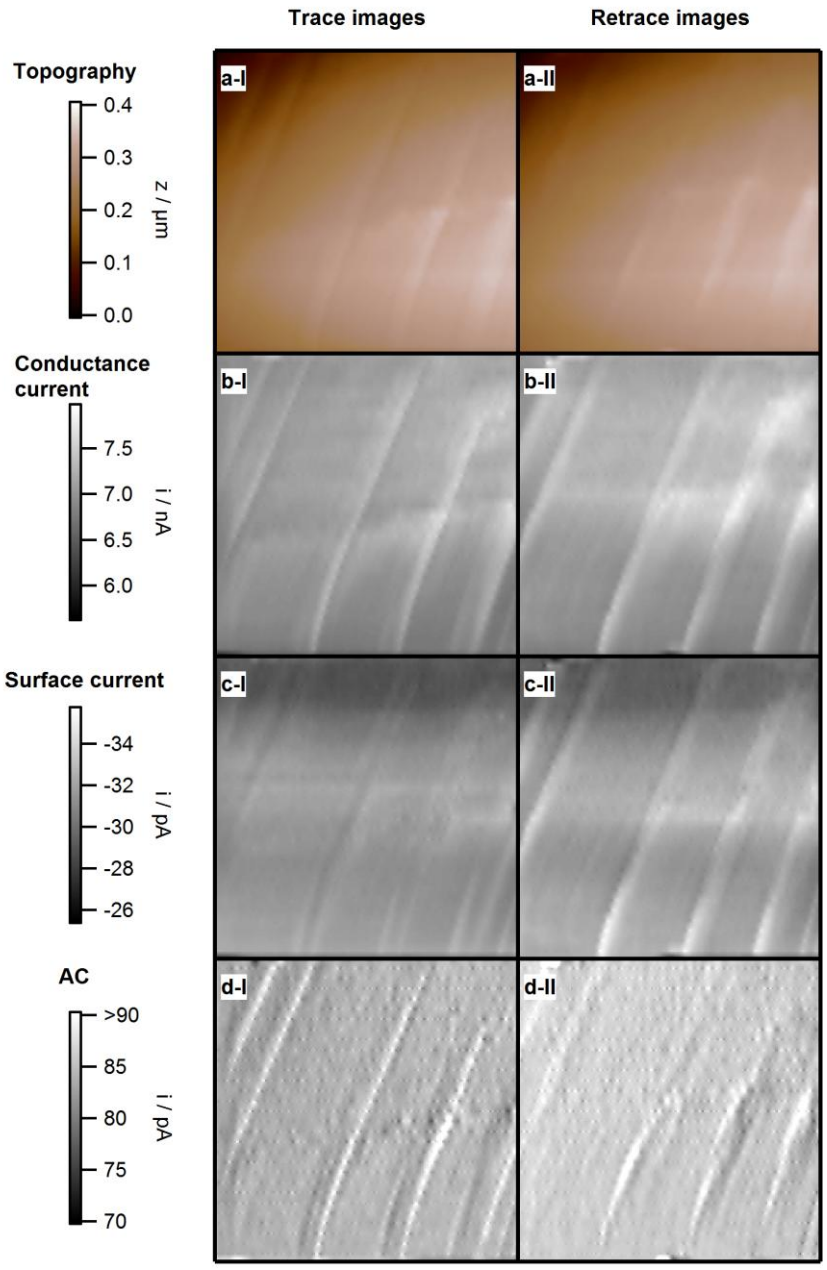

Figure S2.2 Set of SECCM *xy*-maps for the reduction of $Ru(NH_3)_6^{3+}$ obtained during a single experiment. (a) Surface topography. (b) Conductance current between the two QRCEs in the pipet tip. (c) Surface current recorded on the HOPG substrate. (d) Alternating current component of the conductance current, used as a feedback parameter. Images sub-labeled I (left column) refer to forward going (trace) sweeps, recorded from left to right. Images sub-labeled II (right column) refer to backward going (retrace) sweeps, recorded from right to left. The consistency between trace and retrace images is indicative of the stability of the liquid meniscus scanning in different directions and provides further confidence in the data obtained. All images are constructed from 31 line scans from bottom to top, with each line comprising ~1100 recorded data points.

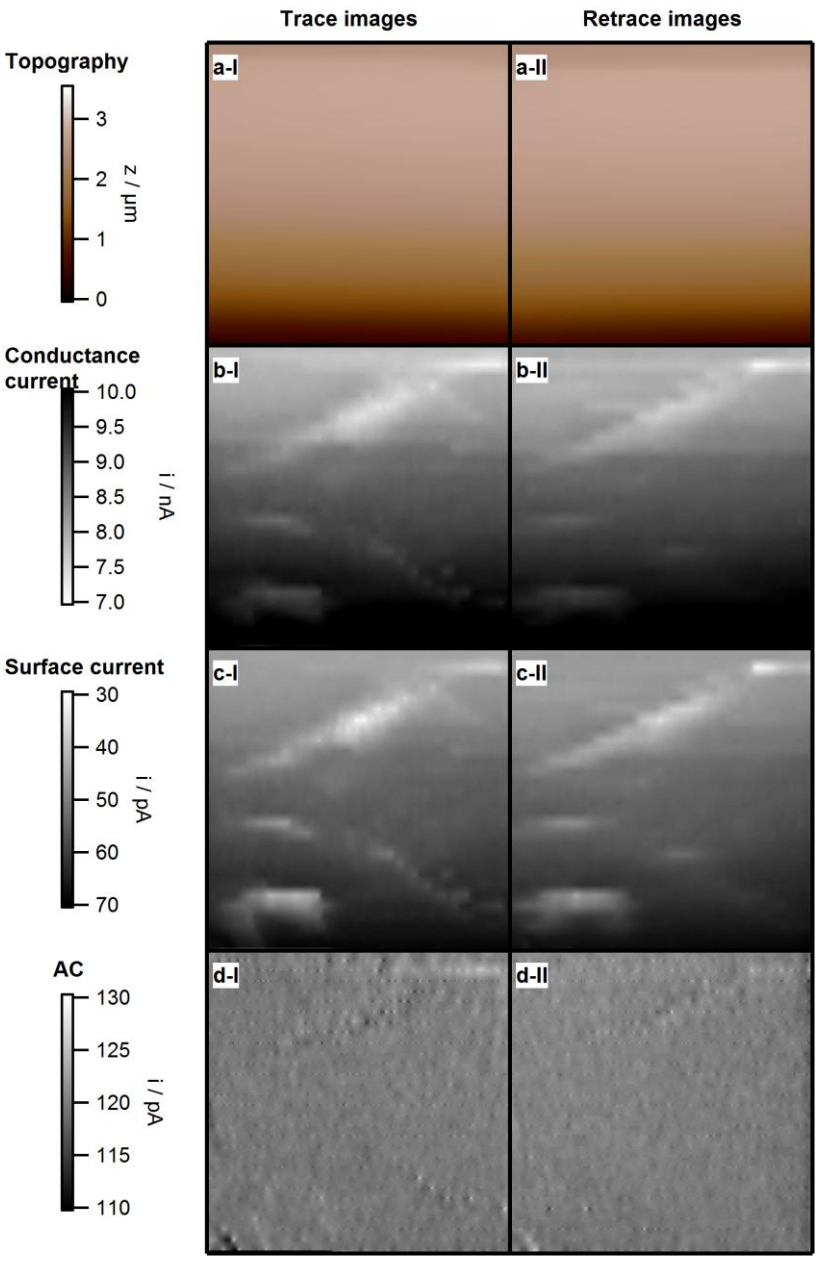

Figure S2.3 Set of SECCM *xy*-maps for the reduction of $Fe(CN)_6^{4-}$ obtained during a single experiment. (a) Surface topography. (b) Conductance current between the two QRCEs in the capillary. (c) Surface current recorded on the HOPG substrate (d). Alternating current component of the conductance current, used as a feedback parameter. Images sub-labeled I (left column) refer to forward going (trace) sweeps, recorded from left to right. Images sub-labeled I (right column) refer to backward going (retrace) sweeps, recorded from right to left. The consistency between trace and retrace images is indicative of the stability of the liquid meniscus scanning in different directions and provides further confidence to the data obtained. All images are constructed from 31 line scans from bottom to top, which each line comprising ~1100 recorded data points.

S.3 ***Linear sweep voltammograms obtained with SECCM***

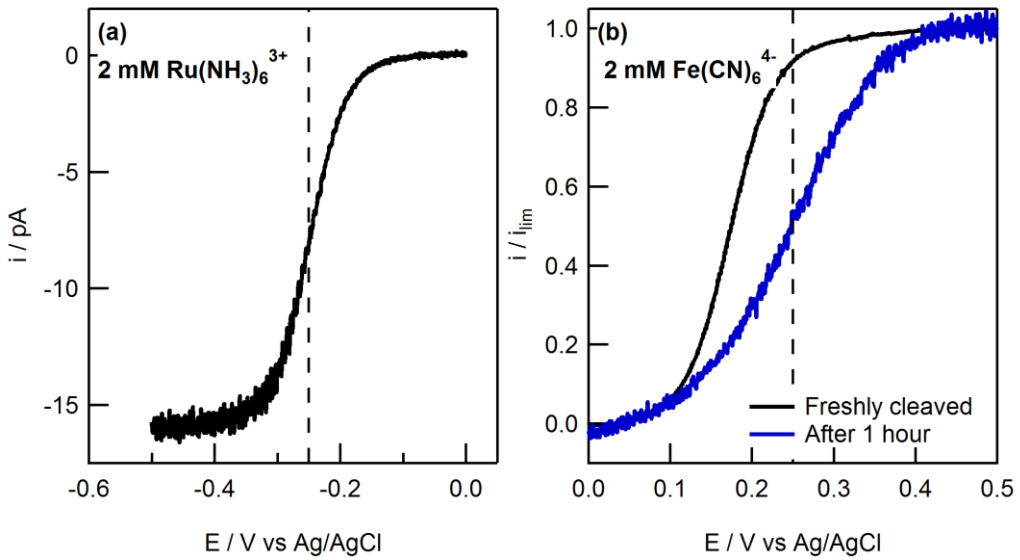

Figure S3 Linear sweep voltammograms (LSVs) obtained with the SECCM set-up in the absence of a potential bias between the QRCEs. (a) LSV for the reduction of 2 mM $Ru(NH_3)_6^{3+}$ (0.1 M KCl). (b) Normalized LSVs for the oxidation of 2 mM $Fe(CN)_6^{4-}$ (0.1 M KCl) on freshly cleaved HOPG (black line) and HOPG after one hour exposure to air (blue line). The LSVs are normalized for comparison as they were obtained with 2 different pipets with different sizes. The position and shape of the waves were found to be representative for a range of pipet sizes (300 nm – 2 μm). The dashed lines indicate the potential at which SECCM images were recorded. The sweep rate for all LSVs was 100 mV s^{-1}. The potential is with respect to Ag/AgCl/(0.1 M KCl).

S.4 Experimental

Materials. Analine, hexaaminеruthenium(III) chloride ($Ru(NH_3)_6Cl_3$, Sigma Aldrich, 98%), potassium ferrocyanide ($K_4Fe(CN)_6$), Fischer Scientific, analytical grade reagent) and potassium chloride (KCl, Sigma Aldrich , "ReagentPlus") were all used as received. All aqueous solutions were prepared from ultra-pure water (Millipore MilliQ, resistivity ca. 18.2 MΩ cm at 25 ºC). Dimethyldichlorosilane ($Si(CH_3)_2Cl_2$, Across Organics, 99+%,) was used to silanize the capillaries.

Methods. AFM images were recorded in tapping mode on a Veeco Multimode AFM. AFM images were processed with the SPIP software package (Image Metrology). FE-SEM images of SECCM tip were acquired with a Zeiss Supra55-VP microscope with the In-Lens detector at 3 kV. SECCM images were processed and analyzed with the Matlab 7.12.0 R2011A (Mathworks) and Igor Pro 6.2.2.2 (Wavemetrics) software packages.

References

(1) (a) Dumitrescu, I.; Unwin, P. R.; Macpherson, J. V. *Chem. Commun.* **2009**, *7345*, 6886-901;
(b) Banks, C. E.; Davies, T. J.; Wildgoose, G. G.; Compton, R. G. *Chem. Commun* **2005**, 829-841;
(c) Bowling, R. J.; Packard, R. T.; Mccreery, R. L. *J. Am. Chem. Soc.* **1989**, *111*, 1217-1223;
(d) Rice, R. J.; McCreery, R. L. *Anal. Chem.* **1989**, *61*, 1637-1641;
(e) Kneten, K. R.; McCreery, R. L. *Anal. Chem.* **1992**, *64*, 2518-2524;
(f) Cline, K. K.; Mcdermott, M. T.; Mccreery, R. L. *J. Phys. Chem.* **1994**, *98*, 5314-5319;
(g) McDermott, M. T.; Kneten, K.; Mccreery, R. L. *J. Phys. Chem.* **1992**, *96*, 3124-3130;
(h) Ji, X.; Banks, C. E.; Crossley, A.; Compton, R. G. *ChemPhysChem* **2006**, *7*, 1337-1344;
(i) Davies, T. J.; Moore, R. R.; Banks, C. E.; Compton, R. G. *J. Electroanal. Chem.* **2004**, *574*, 123-152;
(j) Liu, H.; Favier, F.; Ng, K.; Zach, M. P.; Penner, R. M. *Electrochim. Acta* **2001**, *47*, 671-677;
(k) Xu, J.; Chen, Q.; Swain, G. M. *Anal. Chem.* **1998**, *70*, 3146-3154.
(l) McCreery, R.L. *Chem. Rev.***2008**, *108*, 2646-2687.

(2) (a) Bowling, R.; Packard, R. T.; McCreery, R. L. *Langmuir* **1989**, *5*, 683-688;
(b) Bowling, R. J.; McCreery, R. L.; Pharr, C. M.; Engstrom, R. C. *Analytical* **1989**, *61*, 2763-2766;
(c) Alsmeyer, Y. W.; McCreery, R. L. *Langmuir* **1991**, *7*, 2370-2375;
(d) Robinson, R. S.; Sternitzke, K.; Mcdermott, M. T.; Mccreery, R. L. *J. Electrochem. Soc.* **1991**, *138*, 2412-2418.

(3) Ebejer, N.; Schnippering, M.; Colburn, A. W.; Edwards, M. A.; Unwin, P. R. *Anal. Chem.* **2010**, *82*, 9141-5.

(4) Lai, S. C. S.; Dudin, P. V.; Macpherson, J. V.; Unwin, P. R. *J. Am. Chem. Soc.* **2011**, *133*, 10744-10747.

(5) Shao, Y. H.; Mirkin, M. V. *Anal. Chem.* **1998**, *70*, 3155-3161.